

Decadal variations in Eurasian snow: Relation with Circulation and Possible Influence on Spring Rainfall over China

Zhiyan Zuo¹, Renhe Zhang¹, Song Yang², Wanqiu Wang², Arun Kumar² and Yan Xue²

¹Chinese Academy of Meteorological Sciences, Beijing, China

²Climate Prediction Center, NOAA/NWS/NCEP, Camp Springs, MD, USA

1. Introduction

There has been increasing evidence that the atmosphere influences land surface processes, which in turn affect the atmosphere via feedback mechanisms, particularly at decadal time scales. More than a century ago, Blandford (1884) documented an inverse relationship between winter snow over the Himalayas and subsequent all-India monsoon rainfall. There has been increasing evidence that snow may generate anomalous atmospheric forcing via changing the process of energy and water transfer between land surface and the atmosphere. The existence of snow-monsoon relationship was supported by subsequent studies with updated snow data and numerical models. For example, Wu and Kirtman (2007) showed that the enhanced spring snow cover in western Siberia corresponded to above-normal spring rainfall in southern China. Some studies emphasized the complex nature of the relationship between Eurasian snow and broader-scale Asian monsoon which is also strongly influenced by El Niño-Southern Oscillation (ENSO) and the Arctic Oscillation (AO). However, it has been found that the connection between Asian climate and ENSO is weakening in the recent decades. Several studies reported that Eurasian snow is playing a more important role in Asian climate variations than before.

Here we summarize two recent papers by Zuo *et al.* (2011) that examined the decadal variations in Eurasian snow, focusing on the relation with circulation and the influence on spring rainfall over China.

2. Data and Methods

The present analysis is based on monthly observed rainfall data recorded at 595 stations in China over the period 1958–2004 provided by the National Meteorological Information Centre of China. The monthly snow water equivalent (SWE) dataset (1979–2004) was provided by the National Snow and Ice Center (Armstrong and Brodzik 2005). The monthly mean winds and geopotential heights were obtained from the National Center of Environmental Prediction (NCEP) and the National Center for Atmospheric Research (NCAR) reanalysis version 1 outputs for the period 1948–2006. The 0-month lead (LM0) NCEP Climate Forecast System version 2 (CFSv2) hindcasts, the ensemble of 16 members, were used to investigate the predictability of the relationship between Eurasian SWE and rainfall in China (Saha *et al.* 2010).

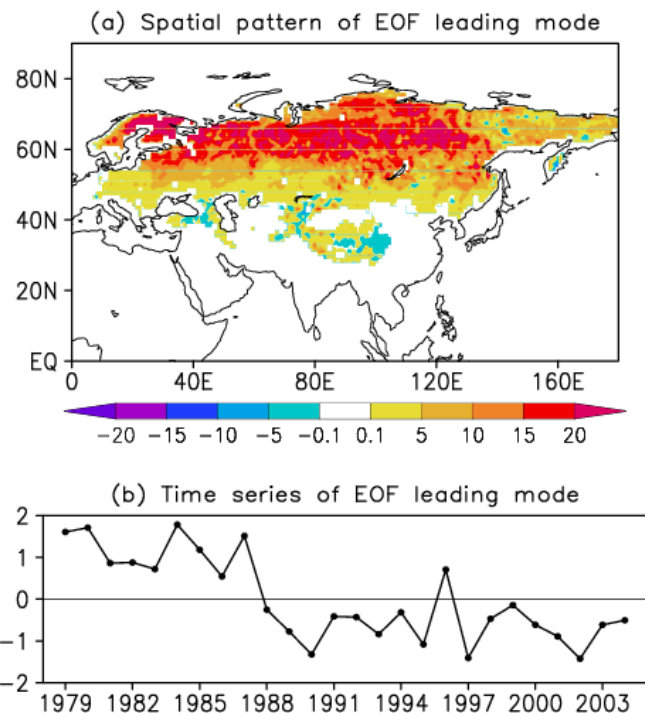


Fig. 1 (a) Spatial pattern of springtime SWE anomalies of the leading mode for the period 1979–2004, and (b) the corresponding time series.

Empirical orthogonal function (EOF) analysis was used to examine the spatial and temporal characteristics of variability in Eurasian SWE ('Eurasia' defined as the domain from 0°E to 180°E, north of 0°N in the present study). In addition, correlation and composite analyses were performed to investigate the relationship between SWE and spring rainfall in China, assessed using Student's *t*-test.

3. Results

Figure 1 shows the first EOF mode of Eurasian spring (March–April–May) SWE and the corresponding time series. The variance percentage explained by the mode is 41.7%. Variation in spring snow in the leading EOF mode is homogeneous over large parts of Eurasia,

with a maximum value of 20 mm in western and central Siberia, whereas the opposite variation is found over small areas such as the region south of Lake Balkhash and the eastern Tibetan Plateau (Fig. 1(a)). The leading mode of the SWE variability shows an apparent decadal shift in the late 1980s, with negative phases during 1988–2004 (hereafter LSWI) and a mainly positive phase during 1979–1987 (hereafter HSWI), which indicates a decreasing decadal trend in spring Eurasian snow from 1979 to 2004 (Fig. 1(b)).

Figure 2(a) shows the climatology of spring rainfall over China for the period 1979–2004. The rainfall shows a gradual increase from northwestern to southeastern China. Precipitation exceeds 300 mm in southeastern China, with a maximum value of 700 mm. To identify the relationship between rainfall in China and spring snow in Eurasian, the composite difference in spring precipitation was calculated between the LSWI and HSWI cases (Fig. 2(b)). Negative differences are seen across most of northwestern China and eastern China, except the Yangtze River valley and parts of Inner Mongolia. The maximum difference, greater than -100 mm, is seen in southeastern China. Figure 2(d) shows the first EOF mode of the spring rainfall anomaly. The first mode is similar to the composite difference between LSWI and HSWI. Note that the variance percentage explained by the mode is 23.5%, demonstrating that the bulk of rainfall variability is explained by decadal variations in Eurasian spring SWE. Figure 2(c) shows the distribution of stations for which the composite differences exceed the 0.1 level of significance. As expected, the composite differences of spring rainfall are significantly negative in southeastern China and positive in southwestern China. Although the difference is small in northern China, spring precipitation shows a significant decrease in southeastern area in Northeast China and a significant increase in northern Inner Mongolia.

Figure 3(a) shows the composite difference of wave activity flux between LSWI and HSWI. Downward and equatorward wave activity flux anomalies appear at mid- and high-latitudes below 200 hPa. The wave activity flux is a three-dimensional extension of the Eliassen–Palm flux (Edmon *et al.* 1980), which reveals the propagation of wave activity and the effect of waves on the flow. Thus, the reduced Eurasian snow acted

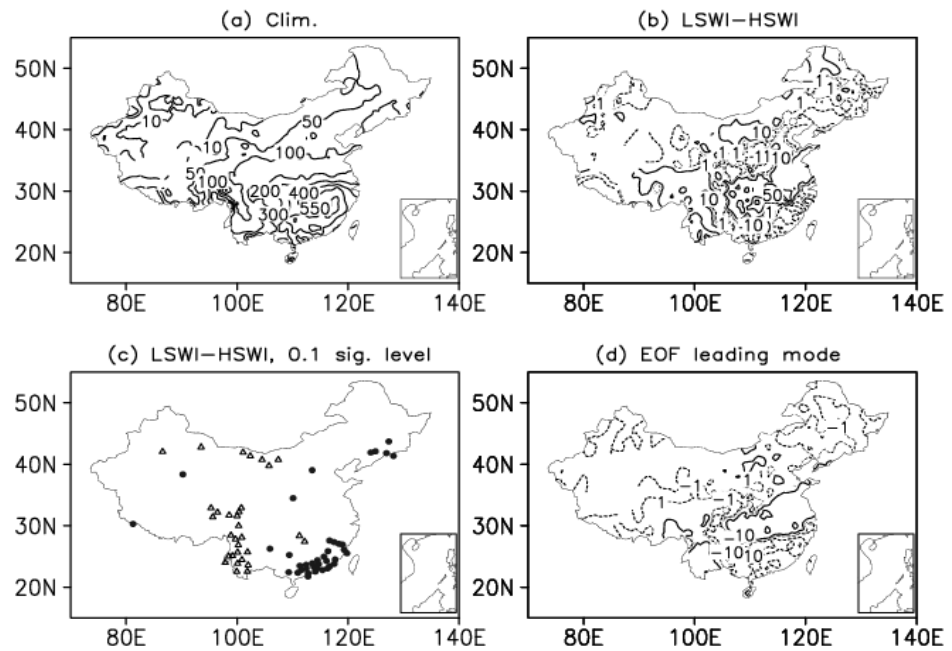


Fig. 2 (a) Climatology of the springtime accumulated precipitation (mm) during 1979–2004, (b) composite difference between the LSWI and HSWI cases, (c) distribution of stations for which the composite difference exceeds the 0.1 level of significance [triangles (dots) indicate significant positive (negative) difference], and (d) the spatial pattern of springtime rainfall anomalies of the leading EOF mode for the period 1979–2004.

to weaken the upward and poleward wave activity flux in the troposphere over Siberia. The center of upward and poleward zonal-mean wave activity flux was also strongly weakened due to reduced snow in Eurasia.

Figure 3(c) shows the composite differences in SLP between LSWI and HSWI. A positive AO phase was associated with decreasing Eurasian snow. A large area of negative anomalies (maximum values exceeding -3 hPa) emerged over the polar cap, extending from Siberia to northern Canada and covering almost the entire polar cap at the land surface. Positive centers appeared in mid-latitude regions, with maximum values exceeding 2 hPa over the North Pacific. The negative SLP anomalies over the Arctic and positive anomalies over mid-latitude areas provided quantitative evidence that deficient snow over the Eurasian continent corresponded to a positive AO phase. The 500-hPa geopotential height field followed a similar pattern to that of SLP.

With a persistent decrease in Eurasian snow, the positive AO phase is associated with anomalous anti-cyclonic circulation over Siberia, resulting in turn in robust northerly anomalies over all of eastern China, with maxima in Northeast and southeastern China (Fig. 3(b)). Consequently, the warm and moist southerly is weakened, resulting in divergence anomalies over Northeast and southeastern China and reduced regional rainfall. In contrast, the northerly anomaly corresponds to greater amounts of water vapor being blocked in southwestern China, resulting in enhanced rainfall. Moreover, the westerly anomaly due to the anomalous anti-cyclone over Siberian is associated with enhanced water vapor convergence over northwestern China, resulting in a positive precipitation anomaly.

The CFSv2 captures the decreasing trend of spring SWE over Eurasia reasonably well (Figure 4(a)), with maximum negative anomalies of -30kg/m^2 in eastern Europe and Siberia. The reduced precipitation over southern China and surrounding oceans is also captured by the CFSv2 successfully, with maximum anomalies -1.2 mm/day over southeastern China (Figure 4(b)). The characteristics aforementioned indicate that the CFSv2 is skillful for predicting the relationships of the Eurasian SWE with the rainfall in southeastern China.

4. Summary and Conclusions

The relationship between decadal variability in spring snow water equivalent (SWE) over Eurasia and spring rainfall over China is investigated using satellite-observed SWE, rainfall observations from 595 stations, and NCEP/NCAR reanalysis data. Decreasing spring SWE in Eurasia corresponded to reduced spring rainfall over southeastern and Northeast China, and more rainfall over southwestern and northwestern China. This relationship was supported by the feedback effect of snow in high-latitude areas to changes in background atmospheric circulation.

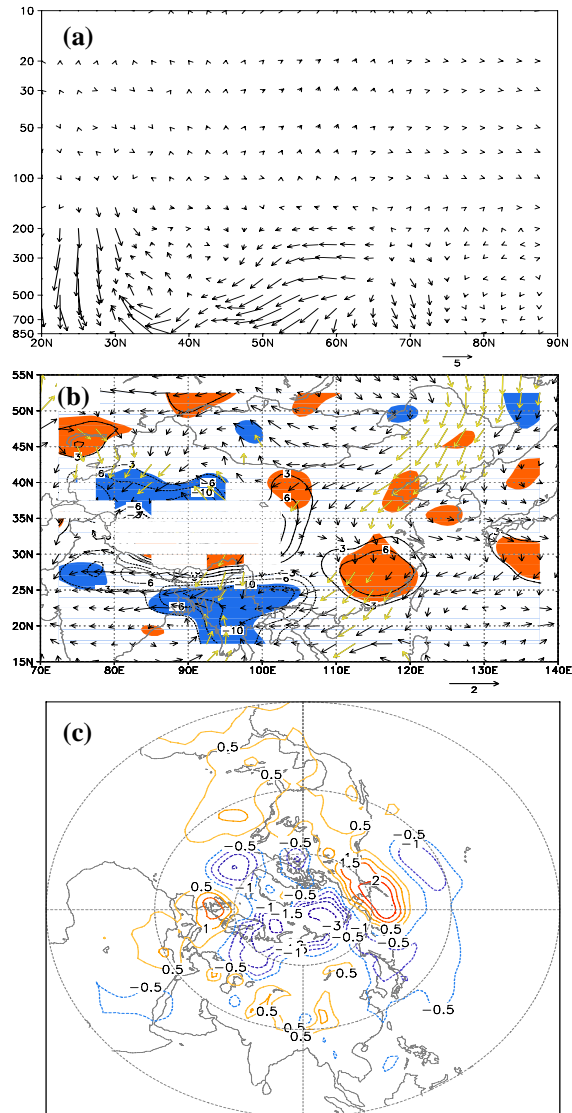


Fig. 3 Composite difference between the LSWI and HSWI cases in terms of meridional and vertical ($\times 10$) wave activity flux ($\text{m}^2 \text{s}^{-2}$) along 90°E (a), the horizontal wind field (vectors, m s^{-1}) and horizontal moisture flux divergence (contours and shading, $\text{g} \times (\text{s} \times \text{cm} \times \text{mb})^{-1} \times 10^{-7}$) at 850 hPa (b) and SLP (c).

A decadal shift in spring Eurasian SWE occurred in the late 1980s, marked by a change from persistent positive phases in 1979–1987 to frequent negative phases. The reduction in Eurasian SWE resulted in reduced upward and poleward wave flux activity, which corresponded to anomalous negative heights/pressures in the Arctic and anomalous positive heights/pressures in mid-latitude regions from the upper-level troposphere to the surface. There was an anomalous anti-cyclonic circulation over Siberia and the western Pacific subtropical high was weakened, accompanied by an anomalous northerly in eastern China and westerly in northwestern China. The anomalous northerly resulted in reduced water vapor convergence in southeastern and Northeast China. Thus, negative rainfall anomalies developed over southeastern and Northeast China, and positive rainfall anomalies appeared over southwestern and northwestern China. Restropective forecasts from CFSv2 successfully simulated the relationship between Eurasian SWE and southeastern China rainfall.

References

- Armstrong, R.L., and M.J. Brodzik, 2005: *Northern Hemisphere EASE-grid weekly snow cover and sea ice extent version 3*. National Snow and Ice Data Center (Boulder, CO, digital media).
- Blanford, H.F., 1884: On the connexion of the Himalaya snowfall with dry winds and seasons of drought in India. *Proceedings of the Royal Society of London*, **37**, 3–22.
- Edmon HJ, Hoskins BJ, McIntyre MF, 1980: Eliassen-Palm crosssections for the troposphere. *Journal of Atmospheric Sciences*. **37**, 2600–2616.
- Saha, S., and Coauthors, 2010: The NCEP Climate Forecast System Reanalysis. *Bull. Amer. Meteor. Soc.*, **91**, 1015–1057.
- Wu, R., and B.P. Kirtman, 2007: Observed relationship of spring and summer East Asian rainfall with winter and spring Eurasian snow. *J. Climate*, **20**, 1285–1304.
- Yang, S., 1996: ENSO–snow–monsoon associations and seasonal–interannual predictions. *Int. J. Climatol.*, **16**, 125–134.
- Zuo, Z., R. Zhang, B. Wu, and X. Rong, 2011: Decadal variability in springtime snow over Eurasia: Relation with circulation and possible influence on springtime rainfall over China. *Int. J. Climatol.*, DOI: 10.1002/joc.2355
- Zuo, Z., Y. Song, W. Wang, A. Kumar, Y. Xue, and R. Zhang, 2011: Relationship between anomalies of Eurasian snow and southern China rainfall in winter. *Environ. Res. Lett.*, **6**, 6pp, DOI: 10.1088/1748-9326/6/4/045402.

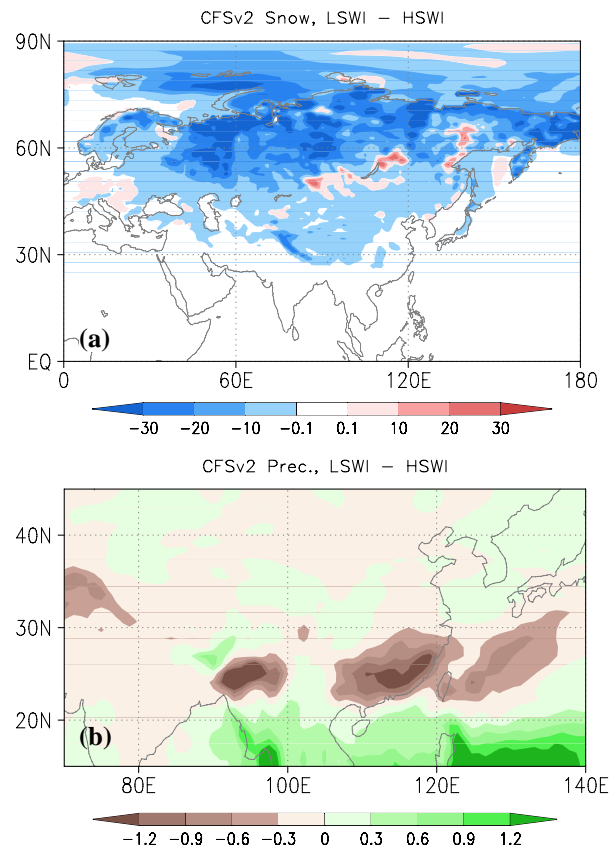


Figure 4 (a) Composite difference between LSWI and HSWI in terms of CFSv2 LMO spring SWE (a) and precipitation (b).